

Energy spectra of donors in GaAs-Ga_{1-x}Al_xAs quantum well structures in the effective-mass approximation

C. Mailhot, Yia-Chung Chang,* and T. C. McGill

California Institute of Technology, Pasadena, California 91125

(Received 22 January 1982; revised manuscript received 14 May 1982)

We present the results of a study of the energy spectrum of the ground state and the low-lying excited states for shallow donors in quantum well structures consisting of a single slab of GaAs sandwiched between two semi-infinite layers of Ga_{1-x}Al_xAs. The effect of the position of the impurity atom within central GaAs slab is investigated for different slab thicknesses and alloy compositions. Two limiting cases are presented: one in which the impurity atom is located at the center of the quantum well (on-center impurity), the other in which the impurity atom is located at the edge of the quantum well (on-edge impurity). Both the on-center and the on-edge donor ground state are bound for all values of GaAs slab thicknesses and alloy compositions. The alloy composition x is varied between 0.1 and 0.4. In this composition range, Ga_{1-x}Al_xAs is direct, and the single-valley effective-mass theory is a valid technique for treating shallow donor states. Calculations are carried out in the case of finite potential barriers determined by realistic conduction-band offsets.

I. INTRODUCTION

The unique nature of electronic states associated with semiconductor superlattices has been the subject of a great deal of interest both from the theoretical¹⁻⁶ and experimental⁷⁻¹⁰ viewpoints. In view of the potential applications of these structures,¹¹⁻¹⁴ the understanding of impurity states found within these systems is an issue of technical as well as scientific importance.

In this paper we report on study of the energy spectrum of shallow donor states in a single GaAs-Ga_{1-x}Al_xAs quantum well, i.e., a structure formed by a central GaAs slab (well material) flanked by two semi-infinite Ga_{1-x}Al_xAs layers (barrier material). The energy spectrum of a donor state located within the GaAs slab is studied as a function of the width of the rectangular potential well formed by the conduction-band offset at the GaAs-Ga_{1-x}Al_xAs interface. The effect of the alloy composition x in the barrier material as well as the position of the donor atom within the well are also investigated. To illustrate the effect of the position of the donor on the electronic spectra, two positions of the donor ion were studied: (1) donor ion at the center of the quantum well (on-center impurity) and (2) donor ion on the edge of the quantum well boundary (on-edge impurity). We find that the donor energy spectrum, both for the on-center and the on-edge impurity, is considerably modified as the dimension of the quantum well is

varied. Both the on-center and the on-edge donor energies with respect to the first conduction sub-band versus GaAs slab thickness present a maximum (in absolute value) whose magnitude depends on the alloy composition. The on-edge impurity produces a more shallow donor ground state than the on-center impurity. This reduction of binding of the on-edge donor ground state results from the fact that the repulsive barrier potential tends to push the electronic charge distribution away from the attractive ionized center thereby leading to a reduced effective Coulomb attraction. This finding is in accord with previous calculations carried in the case of infinite confining potential.¹⁵

In Sec. II we present the calculation techniques. We discuss first the effective-mass Hamiltonian used for treating the shallow states and its validity; then we describe the basis orbitals on which the donor state is expanded. In Sec. III, the main results are presented. First we discuss the energy spectrum for the on-center impurity; then we treat the case of the on-edge impurity. A comparison is made between these two limiting cases. A summary of the results and a conclusion are presented in Sec. IV.

II. CALCULATION METHOD

Calculations are based on the effective-mass approximation (EMA). The GaAs-Ga_{1-x}Al_xAs sys-

tem was chosen since the EMA is known to hold to a high degree of accuracy for shallow donor states in GaAs.¹⁶ As shown by Ando and Mori,¹⁷ the boundary condition that the donor envelope function and the particular current are continuous across the interface is sufficient in the case of GaAs-Ga_{1-x}Al_xAs quantum well structures. For other systems, one would have to go beyond the EMA and use the complex band structure of the superlattice to provide a complete theoretical description of shallow donor states.¹⁸ Since we treat a single quantum well, the results discussed below should apply to superlattices in which the Ga_{1-x}Al_xAs barriers are thick enough so that there is little overlap between the states confined to adjacent GaAs quantum wells. In the case of thin superlattices, one should take into account the spreading of the donor envelope function into the adjacent quantum wells.

The composition of the Ga_{1-x}Al_xAs alloy was varied in the range where the alloy remains direct, so that the single-valley effective-mass theory still holds. Realistic conduction-band offsets of finite magnitude were used, thereby allowing the wave function to penetrate into the barrier material as the dimensions of the confining quantum well are reduced. The use of finite conduction-band offsets has a large effect on the binding energy of the donor state in the thin GaAs slab limit and should be compared with approximate calculations carried out using infinitely high barrier height (quantum box case).^{19,20} For example, as first shown by Levine,²¹ hydrogenic donor states at a semiconductor surface cannot exist unless the sum of the Coulomb quantum numbers, $l + m$, is an odd integer if the potential discontinuity is assumed to be infinite at the surface. In this case, the ground state corresponds to a $2p_z$ hydrogenic state. In particular, spherically symmetric states are not allowed since the donor envelope function is required to vanish at the interface. When finite conduction-band offsets are taken into account, the condition that the wave function vanish at the interface is relaxed and penetration in the barrier material is allowed. The infinite barrier case should be viewed as a limiting case valid only for very wide quantum wells for which the penetration of the donor state into the barrier material is small.

The effective-mass Hamiltonian corresponding to a Coulomb center located at a distance c from the center of a finite quantum well of width $2a$ along the \hat{z} direction (the \hat{z} axis is normal to the interface plane) and height V_0 (see Fig. 1 for geometry) is

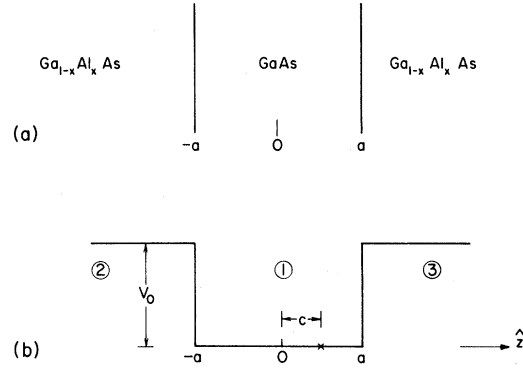


FIG. 1. Geometry of a Coulomb center located at a distance c from the center of a finite quantum well of width $2a$ (along the \hat{z} direction) and height V_0 . (a) Physical structure. (b) Quantum well potential profile along the \hat{z} axis normal to the interfaces.

$$\hat{H}(1) = \frac{-\hbar^2}{2m_1^*} \nabla^2 + V_1(\vec{r}) \quad (1a)$$

in region (1),

$$\hat{H}(2) = \frac{-\hbar^2}{2m_2^*} \nabla^2 + V_2(\vec{r}) + V_0 \quad (1b)$$

in region (2), and

$$\hat{H}(3) = \frac{-\hbar^2}{2m_2^*} \nabla^2 + V_3(\vec{r}) + V_0 \quad (1c)$$

in region (3), where m_1^* refers to the bulk GaAs (well material) effective mass and m_2^* refers to the interpolated effective mass in Ga_{1-x}Al_xAs (barrier material). Since the bulk dielectric constants of GaAs and Ga_{1-x}Al_xAs, ϵ_1 and ϵ_2 , respectively, differ slightly, the Hamiltonian must include terms due to electrostatic image charges.^{22,23} The potentials $V_1(\vec{r})$, $V_2(\vec{r})$, and $V_3(\vec{r})$ represent the Coulomb interaction between the electron and the impurity ion as well as the ion image charge. When the origin is taken to be on the ionized donor, the left and right boundaries of the quantum well are, respectively, $z_0 = -(a+c)$ and $z_0 = (a-c)$. We let the dielectric mismatch between GaAs and Ga_{1-x}Al_xAs be expressed as

$$p \equiv \frac{(\epsilon_1 - \epsilon_2)}{(\epsilon_1 + \epsilon_2)}, \quad (2a)$$

$$p' \equiv \frac{2\epsilon_1}{(\epsilon_1 + \epsilon_2)}, \quad (2b)$$

and the positions of the ion image charges along the \hat{z} axis to be

$$z_0^+(n) = 2 \left\{ \left[n - \left\lfloor \frac{n+1}{2} \right\rfloor \right] (a+c) + \left\lfloor \frac{n+1}{2} \right\rfloor (a-c) \right\}, \quad (3a)$$

$$z_0^-(n) = -2 \left\{ \left\lfloor \frac{n+1}{2} \right\rfloor (a+c) + \left[n - \left\lfloor \frac{n+1}{2} \right\rfloor \right] (a-c) \right\}, \quad (3b)$$

where

$$[x] \equiv \text{int } x. \quad (3c)$$

Letting

$$\rho = (x^2 + y^2)^{1/2} \quad (4a)$$

and

$$r = (\rho^2 + z^2)^{1/2}, \quad (4b)$$

the potential energy in region (1) can be written as

$$V_1(\vec{r}) = \frac{-e^2}{4\pi\epsilon_1} \frac{1}{r} + v_1^+(\vec{r}) + v_1^-(\vec{r}), \quad (4c)$$

where

$$v_1^+(\vec{r}) = \frac{-e^2}{4\pi\epsilon_1} \sum_{n=1}^{\infty} p^n \{\rho^2 + [z - z_0^+(n)]^2\}^{-1/2}, \quad (4d)$$

$$v_1^-(\vec{r}) = \frac{-e^2}{4\pi\epsilon_1} \sum_{n=1}^{\infty} p^n \{\rho^2 + [z - z_0^-(n)]^2\}^{-1/2}, \quad (4e)$$

for the electron-ion potential.

In region (2), the potential energy can be expressed as

$$V_2(\vec{r}) = \frac{-e^2}{4\pi\epsilon_2} p' \sum_{n=0}^{\infty} p^n \{\rho^2 + [z - z_0^+(n)]^2\}^{-1/2}, \quad (4f)$$

for the electron-ion potential.

In region (3), the potential energy can be expressed as

$$V_3(\vec{r}) = \frac{-e^2}{4\pi\epsilon_2} p' \sum_{n=0}^{\infty} p^n \{\rho^2 + [z - z_0^-(n)]^2\}^{-1/2}, \quad (4g)$$

for the electron-ion potential.

A finite number of image charges were included in the expansion of Eqs. (4). Since the dielectric mismatch p is at most of the order of 5% for the $x=0.4$ alloy, the contributions due to higher-order image charge terms are negligible. In the present calculation, we included only four image charge

terms.

The conduction-band offset V_0 was taken to be 85% of the difference of the $\vec{k}=0$ band gaps of GaAs and Ga_{1-x}Al_xAs.²⁴ Since the alloy composition range studied was such that the alloy was direct ($x < 0.45$),²⁴ both the effective mass m_2^* and the conduction-band offset V_0 were determined using the $\vec{k}=0$ values in Ga_{1-x}Al_xAs (Ref. 24):

$$m_1^* = 0.067m_0, \quad (5a)$$

$$m_2^* = (0.067 + 0.083x)m_0, \quad (5b)$$

$$\epsilon_1 = 13.1\epsilon_0, \quad (5c)$$

$$\epsilon_2 = [13.1(1-x) + 10.1x]\epsilon_0, \quad (5d)$$

$$V_0 = 1.06x \text{ eV}, \quad (5e)$$

where m_0 and ϵ_0 are the free electron mass and the vacuum static dielectric constant, respectively.

To calculate binding energies, we must solve for the Hamiltonian defined in Eqs. (1) without the impurity potentials $V_1(\vec{r})$, $V_2(\vec{r})$, and $V_3(\vec{r})$. That is, we must find the ground state of an electron in the quantum well without the impurity potential. The Hamiltonian for the particle in this problem is given by

$$\hat{H}_0(1) = \frac{-\hbar^2}{2m_1^*} \nabla^2 \quad (6a)$$

in region (1),

$$\hat{H}_0(2) = \frac{-\hbar^2}{2m_2^*} \nabla^2 + V_0 \quad (6b)$$

in region (2), and

$$\hat{H}_0(3) = \frac{-\hbar^2}{2m_2^*} \nabla^2 + V_0 \quad (6c)$$

in region (3). The energies (E) of the Coulomb states with respect to the first conduction-subband edge are given by the difference between the donor energy $E(\hat{H})$ and the subband energy $E(\hat{H}_0)$:

$$E = E(\hat{H}) - E(\hat{H}_0). \quad (7)$$

Since the Hamiltonian without the Coulomb center, \hat{H}_0 , is even with respect to reflection through the xy plane, eigenstates of \hat{H}_0 must have definite parity. In particular, eigenstates of \hat{H}_0 belonging to odd-number subbands ($n=1,3,5,\dots$) must be *even* with respect to reflection through the xy plane. Eigenstates of \hat{H}_0 belonging to even-number subbands ($n=2,4,6,\dots$) must be *odd* with respect to reflection through the xy plane.

Calculations were carried out using a variational method. To preserve the cylindrical geometry of the system, the trial basis orbitals on which the donor-state envelope function is expanded are of

$$\langle \vec{r}' | nlm \rangle \equiv \phi_{nlm}(\vec{r}') = \sum_{i=1,2,3} N_i(n,l) [r(\lambda, d_i)]^{l_i} \exp\{-\xi_i(n,l) [r(\lambda, d_i)]^2\} Y_l^m(\Omega'), \quad (8)$$

where $r(\lambda, d_i) \equiv [x^2 + y^2 + \lambda^2(z - d_i)^2]^{1/2}$, and $N_i(n,l)$ is a normalization constant. The index $i=1,2,3$ labels the region of space where the GTO orbital is defined. The boundary conditions that both the wave function and the particle current are continuous across the interface²⁴ determine relations between the normalization constants $N_i(n,l)$ and the orbital exponents, $\xi_i(n,l)$, in the barrier material ($i=2,3$) in terms of those in the well material ($i=1$). To produce an accurate description of the donor envelope wave function, a shape parameter, or eccentricity (λ), as well as a shift parameter (d_i), were incorporated in the variational basis set $\{|nlm\rangle\}$. The shape parameter λ determines the compression of the envelope function along the quantum well axis (\hat{z}). The shift parameter d_i determines the location of the electron charge distribution when the impurity ion is moved towards the quantum well edge. In the calculation presented here we chose (1) $d_i \equiv 0$ in the case of the on-center impurity and (2) $d_0 \neq 0$ for $l=0$ and $d_i=0$ for $l \neq 0$ in the case of the on-edge impurity. The GTO orbital exponents $\xi_1(n,l)$ appearing in Eq. (8) are fixed and taken to be of the form, in atomic rydberg units,²⁵

$$\xi_1(n,l) = \frac{\xi_0}{b(n)(l+1)}, \quad (9)$$

with $b(n) = \{1, 2, 4, 8, 16, 32, \frac{1}{2}\}$ and $\xi_0 = 8/(9\pi)$ bohr⁻². The choice of ξ_0 is dictated by the fact that if one solves the hydrogen-atom Hamiltonian for the ground state with a trial Gaussian orbital of the form $N \exp(-\xi_0 r^2)$, then one easily finds that the orbital exponent ξ_0 that minimizes the expectation value of the energy is $\xi_0 = 8/(9\pi)$ bohr⁻². To make the particle current continuous, we impose continuity of the wave function and of the velocity operator across the quantum well boundary.²⁶ The boundary condition that $(\vec{\nabla} \phi_{nlm} \cdot \hat{z})/m^*$ must be continuous across the interface is required since the difference in effective masses was taken into account in the expression of the Hamiltonian. As shown by Ando and Mori,¹⁷ there are adequate boundary conditions in the case

of the form of Gaussian-type orbitals (GTO's) defined in an ellipsoidal coordinate system and shifted with respect to the ionized donor taken to be at the origin

of GaAs-Ga_{1-x}Al_xAs quantum well structures.

The donor envelope function $|\Psi\rangle$ is expanded on this set of trial orbitals:

$$|\Psi\rangle = \sum_{nlm} C(nlm) |nlm\rangle, \quad (10)$$

where the set of basis orbitals $\{|nlm\rangle\}$ are the ellipsoidal GTO's defined above in Eq. (8).

The problem of solving the EMA Schrödinger equation for the donor envelope function

$$\hat{H}|\Psi\rangle = E(\hat{H})|\Psi\rangle \quad (11)$$

reduces to that of solving the generalized eigenvalue problem

$$\sum_{n'l'm'} [\langle nlm | \hat{H} | n'l'm' \rangle - E(\hat{H}) \langle nlm | n'l'm' \rangle] C(n'l'm') = 0, \quad (12)$$

for the eigenenergy $E(\hat{H})$ and the expansion coefficients $C(nlm)$ appearing in the expansion equation (10).

Calculations were carried out using both s -like ($l=0$) and p -like ($l=1$) GTO's. In the case of the on-center impurity ($c=0$), the Hamiltonian in Eqs. (1) mixes only orbitals whose angular momenta l differ by an even integer. For the on-center impurity, only s -like GTO's were included in the expansion equation (10). However, for the on-edge impurity ($c=a$), the mixing between s - and p -like orbitals becomes appreciable and must be included to provide an accurate description of the neutral donor. For the on-edge impurity, seven s -like GTO's and seven p -like GTO's were included in the expansion equation (10). The calculation of the subband energy $E(\hat{H}_0)$ was carried through using seven s -like GTO's. As mentioned above, eigenstates of \hat{H}_0 belonging to the first conduction subband are even with respect to reflection through the xy plane and thus the donor envelope function can be fairly well described by s -like basis orbitals. For each value of GaAs slab thickness ($2a$), impurity position (c), and barrier height V_0 , the shape parameter λ as well as the shift parameter d_i were

determined by minimizing the energy expectation value in the ground state, $E_0(\lambda, d_l)$.

This shifted ellipsoidal Gaussian set has the advantage of reproducing reasonably well the Coulomb center at both the small ($a \rightarrow 0$) and the large ($a \rightarrow \infty$) slab thickness limit where the binding energy reduces, in the case of the on-center donor, to that of the barrier material or the well material bulk values, respectively. At the same time, it retains the nonspherical character of the problem and allows the basis orbitals to reshape themselves in order to minimize the total energy. The inclusion of a shift parameter d_l in the variational basis set allows the electronic charge distribution associated with the donor ground-state envelope function to be shifted away from the position of the impurity ion. This degree of freedom appears to be most important in the case of the on-edge donor where the Coulomb potential tends to pull the charge distribution towards the ionized center whereas the repulsive barrier potential tends to push it away from the ionized center.

Figure 2 shows the eccentricity (shape parameter λ) for the on-center donor state as a function of the GaAs slab thickness for different alloy composition x . As shown in the figure, greater values of x (i.e., greater conduction-band offset) result in larger shape parameter and therefore tighter GTO's. Furthermore, the shape-parameter—versus—slab-thickness curve presents a maximum corresponding to a maximum confinement of the donor envelope function around the impurity atom. For both very large and very small slab thicknesses, the shape parameter λ reduces to unity as it should in order to describe the isotropic case corresponding to bulk GaAs or bulk Ga_{1-x}Al_xAs, respectively.

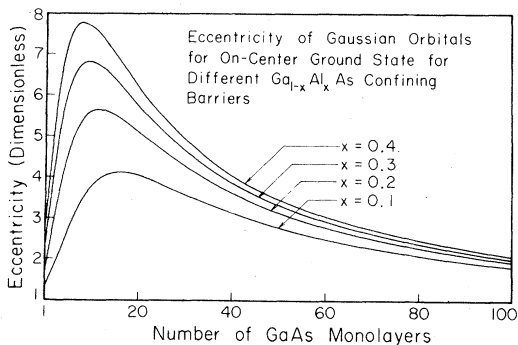


FIG. 2. Eccentricity (shape parameter) λ of ellipsoidal Gaussian type orbitals as a function of GaAs slab thickness for four alloy compositions, $x = 0.1, 0.2, 0.3, 0.4$, of Ga_{1-x}Al_xAs.

III. RESULTS

We first treat the results obtained for the on-center impurity case ($c = 0$). Then we treat the on-edge impurity case ($c = a$). Comparisons are made between these two limiting cases.

Figure 3 shows the on-center donor ground-state envelope function through the Coulomb center and normal to the interface plane for the different GaAs slab thicknesses and alloy compositions. Greater Al composition produces higher conduction-band offsets which, in turn, tend to localize the donor envelope function more effectively. As shown in Fig. 3, for very thin GaAs slab, the envelope function leaks appreciably into the barrier material (Ga_{1-x}Al_xAs). In the limit of very thin GaAs slab thicknesses, one should recover the binding energy corresponding to bulk Ga_{1-x}Al_xAs. Conversely, for large GaAs slab thicknesses, the on-center donor ground state is mostly confined within the quantum well and one

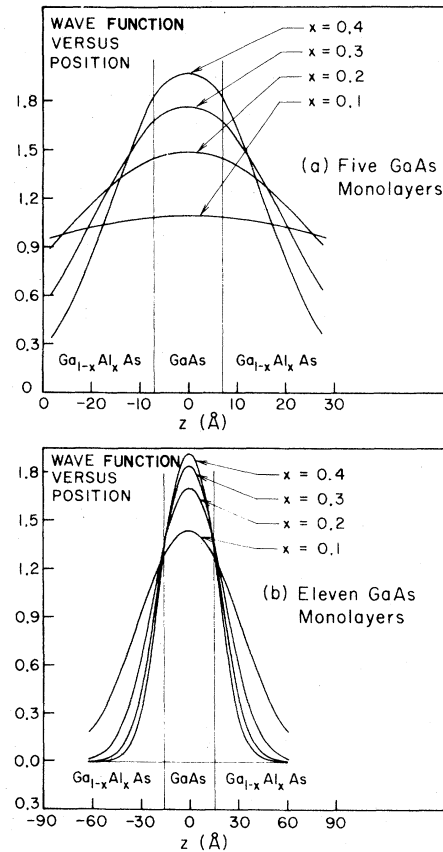


FIG. 3. On-center donor ground-state envelope function plotted along the axis normal to the interfaces for different GaAs slab thicknesses and four alloy compositions, $x = 0.1, 0.2, 0.3, 0.4$, of Ga_{1-x}Al_xAs.

should recover the binding energy for bulk GaAs. As mentioned above, the EMA Hamiltonian for the on-center impurity mixes only orbitals whose angular momenta l differ by an even integer. As shown in Fig. 3, the total on-center impurity wave function does not acquire a p -like character.

Figure 4 shows the energy, with respect to the first conduction subband, for the on-center donor ground state as a function of GaAs slab thickness for four alloy compositions, $x=0.1, 0.2, 0.3, 0.4$. For the on-center impurity, the energy with respect to the first conduction subband versus GaAs slab thickness presents a maximum (in absolute value) whose magnitude depends on the alloy composition of the barrier material. Greater Al composition in the barrier material leads to larger conduction-band offsets and therefore more complete confinement of the donor envelope function. Since greater confinement of the donor state leads to a more sharply peaked wave function as the envelope function builds up amplitude around the impurity ion, the attractive Coulomb potential is more effective in binding the donor state when the Al content in the $\text{Ga}_{1-x}\text{Al}_x\text{As}$ barrier is increased. For large GaAs

slab thicknesses, the effect of the alloy composition x or, equivalently, of the barrier height V_0 , on the on-center donor ground-state energy and wave function is greatly reduced since the envelope function is strongly localized around the impurity ion in the center of the quantum well and does not feel much the repulsive barrier potential.

Figure 5 shows the energy, with respect to the first conduction subband, for the on-center low-lying excited states of even parity as a function of GaAs slab thickness for four alloy compositions, $x=0.1, 0.2, 0.3, 0.4$. The qualitative dependence of the GaAs slab thickness on the energy with respect to the first conduction subband of the even-parity excited states is similar, though not as important, to that of the ground state as can be seen by comparing Figs. 4 and 5. The envelope functions corresponding to these excited states are even with respect to reflection through the xy plane since these are made up from states derived from the first conduction subband.

Figure 6 shows the on-edge donor ground-state envelope function through the Coulomb center and normal to the interface plane. As mentioned

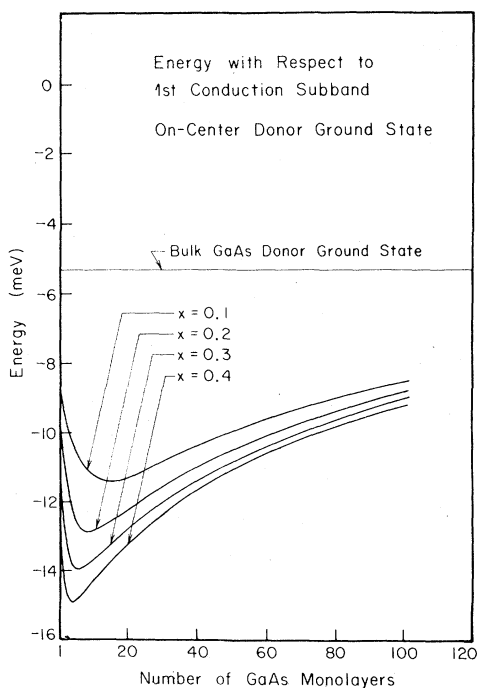


FIG. 4. Energy of the on-center donor ground state with respect to the first conduction subband as a function of GaAs slab thickness for four alloy compositions, $x=0.1, 0.2, 0.3, 0.4$, of $\text{Ga}_{1-x}\text{Al}_x\text{As}$. Calculations are carried through using seven s -like ellipsoidal Gaussian-type orbitals as defined in the text.

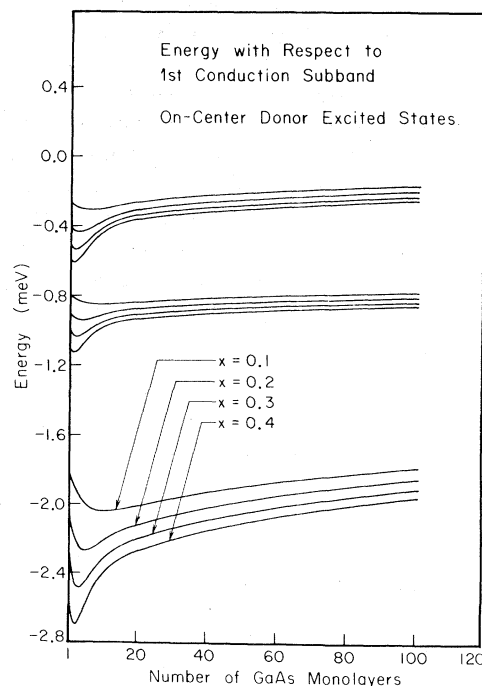


FIG. 5. Energy of the on-center low-lying excited states of even parity with respect to the first conduction subband as a function of GaAs slab thickness for four alloy compositions, $x=0.1, 0.2, 0.3, 0.4$, of $\text{Ga}_{1-x}\text{Al}_x\text{As}$. Calculations are carried through using seven s -like ellipsoidal Gaussian-type orbitals as defined in the text.

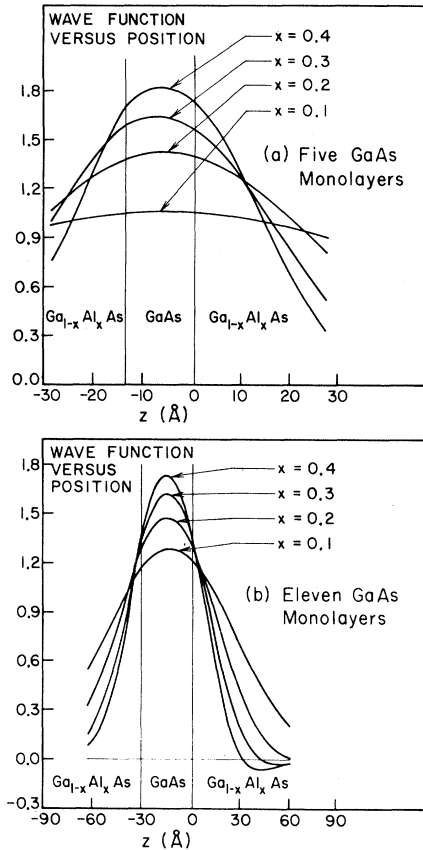


FIG. 6. On-edge donor ground-state envelope function plotted along the axis normal to the interfaces for different GaAs slab thicknesses and four alloy compositions, $x=0.1, 0.2, 0.3, 0.4$, of Ga_{1-x}Al_xAs.

above, although the on-center donor wave function is entirely s -like, the on-edge wave function develops a strong p -like character. The p -like character of the on-edge wave function increases as the height of the conduction-band offset V_0 increases.

Figure 7 shows the energy, with respect to the first conduction subband, of the on-edge donor ground state as a function of the GaAs slab thickness for four alloy compositions, $x=0.1, 0.2, 0.3, 0.4$. The on-edge donor energy curve presents qualitatively the same features as the on-center donor energy curve. In the thin GaAs slab limit, the energy curves for the on-center and the on-edge donor are very similar. In the thick GaAs slab limit, the on-edge donor is less tightly bound than the on-center donor. This is mainly due to the fact that, as the impurity ion approaches the quantum well edge, the donor ground-state envelope function should be constructed more and more from Bloch states derived from the Ga_{1-x}Al_xAs conduction-

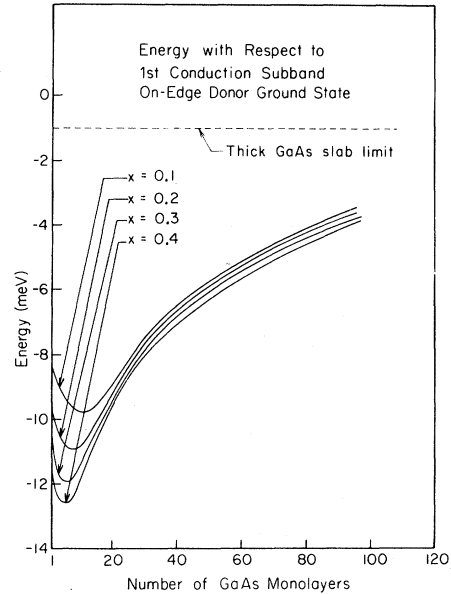


FIG. 7. Energy of the on-edge donor ground state with respect to the first conduction subband as a function of GaAs slab thickness for four alloy compositions, $x=0.1, 0.2, 0.3, 0.4$, of Ga_{1-x}Al_xAs. Calculations are carried through using seven s -like and seven p -like ellipsoidal Gaussian-type orbitals as defined in the text. The dashed line indicates that energy with respect to the first conduction subband in the large GaAs slab-thickness limit.

band edge. These states lie above the GaAs conduction-band edge by an energy equal to the conduction-band offset between GaAs and Ga_{1-x}Al_xAs. As the on-edge donor ground-state envelope function includes more of these higher-energy states, the on-edge donor ground state becomes more shallow than the on-center donor ground state. Furthermore, in the case of the on-edge center, the repulsive barrier potential tends to push the electronic charge distribution away from the ionized donor, leading to a reduced Coulomb attraction. For the on-edge impurity, the results presented here using finite conduction-band offsets are qualitatively similar to the case where infinite conduction-band offsets are assumed,¹⁵ thereby preventing the donor envelope function from leaking out of the quantum well. The dashed line in Fig. 7 indicates the binding energy in the limit of large GaAs slab. The boundary conditions on the wave function at the interface in the finite conduction-band offset case gives the donor envelope function a d -like character as the slope of the wave function is vanishingly small on the donor center. In the large slab limit, the p -like character of the

donor envelope function is less important for the finite conduction-band offset case and the donor ground state mostly consists of shifted *s*-like orbitals.

IV. SUMMARY AND CONCLUSION

We have calculated the energy spectrum of shallow donor states in GaAs-Ga_{1-x}Al_xAs quantum well structures using the effective-mass approximation scheme. The variation in energy with respect to the first conduction subband of the donor ground state and the low-lying excited states was studied as a function of the central GaAs slab thickness, the position of the impurity atom within the GaAs slab and the alloy composition *x* of Ga_{1-x}Al_xAs. Calculations were done for four alloy compositions of Ga_{1-x}Al_xAs in a range in which the alloy remains direct (*x* < 0.45). Realistic values for conduction-band offsets of finite magnitude were used. The effect of the impurity position on the binding energy of the donor state was investigated in the two limit cases where the impurity ion was at the center of the quantum well (on-center impurity) and at the edge of the quantum well (on-edge impurity).

In the case of both the on-center and the on-edge impurities, the energy with respect to the first conduction subband versus slab thickness presents a maximum (in absolute value) corresponding to a maximum confinement of the donor-state envelope wave function. In the case of the on-edge impurity, the donor ground state is not as tightly bound

as the on-center ground state. The reduction in the binding for the on-edge impurity is a direct consequence of the repulsive interface potential which tends to push the electronic charge distribution away from the Coulomb center.

For both the on-center and the on-center impurity, it was found that the energy spectrum of the donor ground state and the low-lying excited states is considerably modified as the thickness of the GaAs slab containing the impurity was varied. This variation in binding energy should be easily observed experimentally since molecular-beam epitaxy techniques²⁷ now allow for the fabrication of superlattices consisting of alternating slabs of few monolayers of GaAs-Ga_{1-x}Al_xAs. It seems possible to adjust the binding of a Coulomb center in a superlattice by varying the thickness of the slab containing the impurity center.

ACKNOWLEDGMENTS

This work was supported by the Army Research Office under Contract No. DAAG29-80-C-0103. One of us (C.M.) has been supported by the National Science and Engineering Research Council (NSERC) of Canada and by the Fonds F.C.A.C. pour l'aide et le soutien à la recherche of Québec. The authors are greatly indebted to G. Bastard and to F. Stern for pointing out the deficiencies of a previous calculation using a less adequate variational basis set than the one presented here. The authors also wish to acknowledge C.A. Swarts for many very helpful discussions.

*Present address: Department of Physics, University of Illinois, Urbana, Illinois 61801.

¹J. N. Schulman and T. C. McGill, Phys. Rev. Lett. **39**, 1680 (1977).

²R. N. Nucho and A. Madhukar, J. Vac. Sci. Technol. **15**, 1530 (1978).

³J. N. Schulman and T. C. McGill, Phys. Rev. B **19**, 6341 (1979).

⁴D. Mukherji and B. R. Nag, Phys. Rev. B **12**, 4338 (1975).

⁵G. A. Sai-Halasz, L. Esaki, and W. A. Harrison, Phys. Rev. B **18**, 2812 (1978).

⁶S. Satpathy and M. Alterelli, Phys. Rev. B **23**, 2977 (1981).

⁷R. Dingle, W. Wiegmann, and C. Henry, Phys. Rev. Lett. **33**, 827 (1974).

⁸R. Tsu, A. Koma, and L. Esaki, J. Appl. Phys. **46**, 842 (1975).

⁹Y. Guldner, J. P. Vieren, P. Voisin, M. Voos, L. L. Chang and L. Esaki, Phys. Rev. Lett. **45**, 1719 (1980).

¹⁰L. L. Chang, H. Sakaki, C. A. Chang, and L. Esaki, Phys. Rev. Lett. **38**, 1489 (1977).

¹¹L. Esaki and R. Tsu, IBM J. Res. Develop. **14**, 61 (1970).

¹²R. Dingle, H. L. Strörmer, A. C. Gossard, and W. Wiegmann, Appl. Phys. Lett. **33**, 665 (1978).

¹³J. N. Schulman and T. C. McGill, Appl. Phys. Lett. **34**, 663 (1979).

¹⁴J. P. van der Ziel, R. Dingle, R. C. Miller, W. Wiegmann, and W. A. Nordland Jr., Appl. Phys. Lett. **26**, 463 (1975).

¹⁵G. Bastard, Surf. Sci. **113**, 165 (1982).

¹⁶G. E. Stilman, C. M. Larsen, C. M. Wolfe, and C. R. Brandt, Solid State Commun. **9**, 51 (1967).

¹⁷T. Ando and S. Mori, Surf. Sci. **113**, 124 (1982).

- ¹⁸J. N. Schulman and Y. C. Chang, *Phys. Rev. B* **24**, 4445 (1981).
- ¹⁹P. Voisin, G. Bastard, C. E. T. Gonçalves da Silva, M. Voos, L. L. Chang, and L. Esaki, *Solid State Commun.* **39**, 79 (1981).
- ²⁰R. C. Miller, D. A. Kleinman, W. T. Tsang, and A. C. Gossard, *Phys. Rev. B* **24**, 1134 (1981).
- ²¹J. D. Levine, *Phys. Rev.* **140**, A586 (1965).
- ²²B. V. Pethukov, V. L. Pokrovskii, and A. V. Shaplik, *Fiz. Tverd. Tela (Leningrad)* **9**, 70 (1967) [*Soviet Phys.—Solid State* **9**, 51 (1967)].
- ²³N. O. Lipari, *J. Vac. Sci. Technol.* **15**, 1412 (1978).
- ²⁴H. C. Casey and M. B. Panish, *Heterostructure Lasers* (Academic, New York, 1978), Part A, Chap. 4.
- ²⁵Atomic units are defined here with respect to GaAs bulk values. Energy is measured in units of $(m_1^* e^4)/(2\hbar^2 \epsilon_1^2)$ (donor rydberg) and distance is measured in units of $(\hbar^2 \epsilon_1)/(m_1^* e^2)$ (donor bohr). The effective mass m_1^* and the static dielectric constant ϵ_1 both refer to GaAs bulk values.
- ²⁶W. A. Harrison, *Phys. Rev.* **123**, 85 (1961).
- ²⁷A. C. Gossard, P. M. Petroff, W. Wiegmann, R. Dingle, and A. Savage, *Appl. Phys. Lett.* **29**, 323 (1976).